^{13}C NMR study of the director distribution adopted by the modulated nematic phases formed by liquid-crystal dimers with odd numbers of atoms in their spacers

J. W. Emsley,[1,*] M. Lelli,[2,†] G. R. Luckhurst,[1,‡] and H. Zimmermann[3,§]

[1]*Chemistry, University of Southampton, Highfield, Southampton, SO17 1BJ, United Kingdom*

[2]*Department of Chemistry, Center for Magnetic Resonance, University of Florence, Sesto Fiorentino (FI) 50019, Italy*

[3]*Max-Planck-Institut für Medizinische Forschung, Department of Biomolecular Mechanisms, D-69120 Heidelberg, Germany*

(Received 28 June 2017; published 15 December 2017; corrected 7 February 2018)

The orientational order of the molecules in the bent mesogen CB6OCB has been studied throughout the range of temperature stability of both the N_U and N_{TB} liquid-crystal phases by ^{13}C NMR spectroscopy. These spectra provide local order parameters for the *para* axes of both of the nonequivalent cyanobiphenyl groups and show how they change on entering the twist-bend nematic phase. A key feature of the order parameters is a weak, but clear maximum in the temperature variation of the order parameter prior to the N_{TB} phase. This suggests that the directors in both the N_U and N_{TB} phases are tilted with respect to the magnetic field of the spectrometer. Significantly the conformational states of the spacer are comparable in both phases, although the low temperature nematic is chiral but not that at high temperature. It is proposed that the higher temperature, tilted phase could be the splay-bend nematic phase.

DOI: 10.1103/PhysRevE.96.062702

I. INTRODUCTION

Molecules which have chiral centers or shape can form enantiomorphic, solid crystals, but the converse is not true. This statement was first verified in the mid-19th century [1], but was not discovered for a fluid phase, a liquid crystal, until 1997 when it was shown by Sekine *et al.* [2] that an enantiomorphic Sm-*C* phase was formed by an achiral molecule. The compound forming this unusual phase was described as being a "bent-core or banana mesogen," because it possessed a semirigid, central core with a bent shape. In 2001 Dozov [3] suggested that a nematic phase formed from achiral molecules having this shape might have a negative value for the elastic constant K_{33} and would form a nematic phase in which the directors, defined as the symmetry axis of second-rank tensorial properties at a particular point in the sample [4], form a helicoidal arrangement as sketched in Fig. 1. Such a nematic phase would be enantiomorphic, and could exist in domains having either *P* or *M* helicity with equal probability. Note that in contrast with the helical arrangement of directors in a chiral nematic phase, N^*, the pitch of these helices is predicted and found to be of the order of a few molecular lengths.

Dozov named this proposed new phase as a twist-bend nematic phase, N_{TB}, which he predicted could exist at a lower temperature than a normal uniaxial nematic phase, and would have the same uniaxial symmetry about the local directors and the helix axis. There is a growing number of compounds which have been shown to exhibit this sequence of two, uniaxial nematic phases, and some common features of these systems have emerged [5–11]. First, a bent structure of the whole molecule is mandatory, which may be caused by the presence in the molecule of a rigid, or semirigid, bent core, or may occur because semirigid fragments are linked by a more flexible chain. The latter are mostly symmetric liquid-crystal dimers of the type shown in Fig. 2.

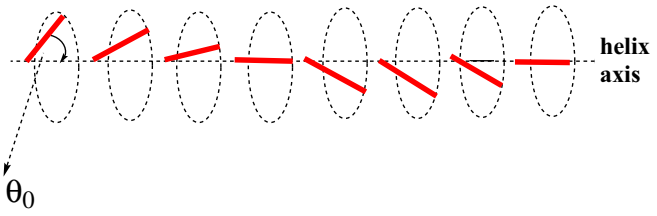

FIG. 1. The formation of tilted directors (red) into a helix in the twist-bend nematic phase. The directors are at a constant tilt, or conical angle θ_0, with respect to the helix axis.

The central chain, or spacer, -$(CH_2)_n$-, confers a bent structure to the whole molecule when *n* is odd independently of whether the linking chain is in a fixed, minimum-energy conformation, or exists as a distribution of many conformations. Note that the angle between the two aromatic arms is suggested by theory [12] to be limited to a range of about 15°.

Second, both nematic phases appear to have uniaxial symmetry. In the higher temperature nematic, N_U, the symmetry about each local director at a point *i*, $\mathbf{d}_i$, is created by anisotropic, rotational motion of the molecules, which together with the apolar character of the distribution of molecular orientations relative to the plane normal to $\mathbf{d}_i$ produces a phase with symmetry $D_{\infty h}$. In addition to these molecular motions relative to the local directors there is also, in the N_{TB} phase, diffusion along each helix axis in a single domain which makes the total phase symmetry S_2 relative to this axis.

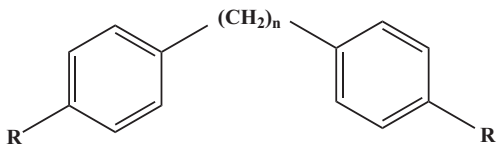

FIG. 2. Symmetric liquid-crystal dimers.

*jwe@soton.ac.uk
†moreno.lelli@unifi.it
‡G.R.Luckhurst@soton.ac.uk
§Herbert.Zimmermann@mpimf-heidelberg.mpg.de

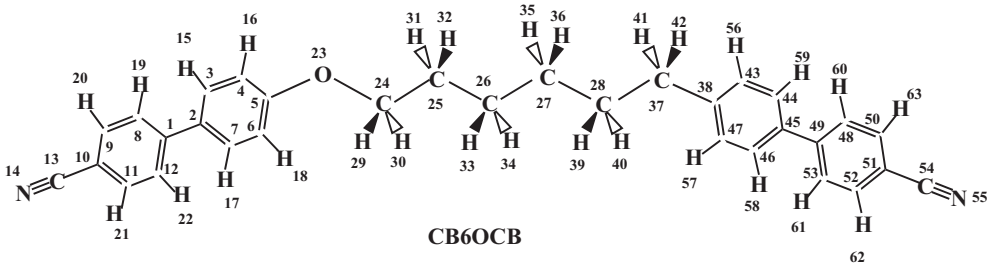

FIG. 3. The nonsymmetric liquid-crystal dimer CB6OCB.

Third, as expected, the local directors, $\mathbf{d}_i$, can be aligned uniformly by an applied magnetic field of intensity B in the N_U phase. Uniform alignment has also been achieved in the N_{TB} phase by fields of 7.05 T [6], but now it is the helix axes which are aligned [13]. Uniform alignment is not achieved at values of $B = 0.3$ T, as evidenced by electron spin resonance (ESR) experiments [6]. It is not yet clear what the minimum value of B is to produce a uniform alignment of the helix axis in the N_{TB} phase.

It has been claimed recently by a study on a number of symmetric dimers, which show the phase sequence Cr-N_{TB}-N_U-I, that the transition temperatures between each of these phases increased significantly in the presence of a magnetic field on increasing the value of B from 0 to 24 T [14]. It was suggested, as a possible explanation of this phenomenon, that the magnetic field can increase the angle between the two semirigid, mesogenic groups of the dimers, so decreasing the molecular curvature or anisotropy.

Fourthly, for some mesogens having the phase sequence N_{TB}-N_U and a long N_U range [15], the orientational order parameter, S_{zz}, for the *para* axes of the semirigid arms measured relative to the applied magnetic field in NMR experiments increases as the temperature is decreased from T_{NI}. The value of S_{zz} reaches a maximum and then decreases until the enantiomorphic nematic phase is reached at $T_{N_{TB}N_U}$, when there is a small discontinuous decrease and S_{zz} then decreases throughout the N_{TB} phase. The unusual temperature dependence of the order parameter S_{zz} indicates that the directors in the N_U phase develop a tilt with respect to the applied magnetic field direction, which suggests that this is a different kind of nematic phase from those observed for approximately linear mesogens.

The most striking property of the N_{TB} phase is that it is enantiomorphic, and in the model of Dozov this is attributed to the helicoidal structure adopted by the local directors originating from the negative bend elastic constant, K_{33}. An alternative suggestion is that the individual molecules spontaneously become chiral on entering the N_{TB} phase through a suitable structural or conformational change [16,17]. Testing these two hypotheses is perhaps the most important aim of experimental studies. As yet there has been just one such study [18], which concluded that the conformational distribution and structure were approximately the same in both nematic phases for the symmetric dimer CB7CB.

Most studies of mesogens which show two nematic phases attribute the low temperature, enantiomorphic phase as being the twist-bend nematic with directors distributed helicoidally, but there are dissenting opinions in which this phase is often described as an N_X phase, to indicate that the structure was not known. For example, the distribution of the directors in the N_{TB} phase of CB11CB has been investigated by ESR spectroscopy of a dissolved nitroxide free radical spin probe. The spectra obtained have been interpreted as being inconsistent with the Dozov model [19]. An ESR study of electron-spin-doped CB7CB [6] noted a similar discrepancy, but attributed this to a nonuniform distribution within the sample of the director with respect to the magnetic field.

Examples of compounds which form the N_{TB} phase continue to be synthesized and to be studied by various physical techniques. Most of these are symmetric dimers but recently a nonsymmetric dimer, CB6OCB, Fig. 3, has been studied and characterized in some detail [20]. It has the following phase sequence: Isotropic $\rightarrow$ 153 °C nematic $\rightarrow$ 109 °C twist-bend nematic $\rightarrow$ 100 °C crystal, with the transitional entropies, $\Delta S/R$, of 0.11(N-I)and 0.018 (N_{TB}-N). The wide nematic phase makes this a particularly attractive compound to study. For example, the orientational order parameter for the difluoroterphenyl group in the symmetric dimer, DTC5C9, Fig. 4, which has the same sequence of liquid-crystal phases, and a N_U range of similar width, has a very unusual temperature profile [15], and a similar order parameter temperature dependence has been observed for a liquid-crystal mixture, also having the same sequence of phases [21].

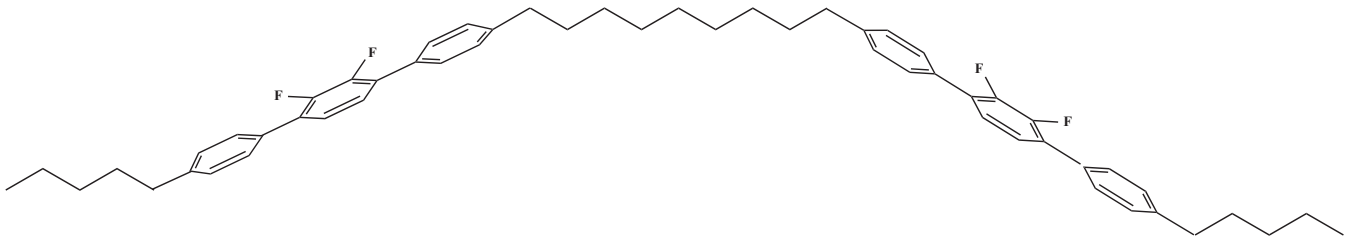

FIG. 4. The symmetric liquid-crystal dimer DTC5C9.

The order parameters for DTC5C9 were obtained by measuring at each temperature the chemical shift, δ_i(LC), of a ^{13}C nucleus present at natural abundance in the mesogen, in the liquid-crystal phase, and comparing it with $\delta_i(I)$, the chemical shift of the same nucleus at a temperature in the isotropic phase. These chemical shifts are very easily measured with good precision from ^{13}C-{^{1}H} NMR spectra, and the same technique will be used here to obtain the temperature profile of order parameters S_{zz}(ArC) and S_{zz}(ArO) for the z axes (*para* axes) of the cyanobiphenyl group attached to the aliphatic chain via either carbon or oxygen. The sample of CB6OCB that was investigated in these studies was prepared in the Max-Planck-Institut für Medizinische Forschung, Heidelberg, using the synthetic procedure described in the Supplemental Material associated with Ref. [20].

The layout of our paper is as follows. In the next section the application of ^{13}C-NMR spectroscopy to the detailed study of the dimer is described. Of special importance are the ^{13}C-{H} shifts discussed in Sec. III. The assignments of the chemical shifts to particular carbon atoms in CB6OCB are addressed in Sec. IV. The variation of the chemical shift anisotropy with temperature, of special significance to the measurement of the orientational order, is described in Sec. V. The determination of the orientational order parameters for particular rigid fragments of the cyanobiphenyl groups is described in Secs. VI and VII. The following Sec. VIII describes the important task of determining and understanding the conical angle in the N_{TB} phase and the tilt angle in the N phase. The conformational distribution for the aliphatic carbon atoms of the central spacer is described in Sec. IX and that of the bond rotations in Sec. X. Our conclusions are given in Sec. XI together with a summary of our key results.

II. NMR EXPERIMENTS

Proton-decoupled, carbon-13 spectra were obtained on a 500 MHz (11.7 T) Bruker spectrometer at the High Field Laboratory in Lyon. The sample was contained in a glass tube with an internal diameter of ~2 mm, and was ~10 mm in length. Heating was by a stream of N_2 gas, with the temperature monitored by a thermocouple located close to but outside of the sample. The setting of the temperature, and maintaining it constant, was achieved with a Bruker Extreme controller. The difference, ΔT, between the temperature set by the controller and that inside the sample was determined by recording ^{1}H spectra as the sample was heated through the N_{U} to the isotropic phase transition. The ^{1}H spectra change dramatically as the samples pass through this transition (for an example, see [15]). Assuming that T_{NI} is identical to that obtained for the sample outside the spectrometer yielded $\Delta T = 9 \pm 1\,^{\circ}$C. The ^{13}C-{^{1}H} spectra are sensitive to changes between crystal-N_{TB}, N_{TB}-N_{U}, and N_{U}-I, and in each case the transition temperatures measured by NMR agreed to within ~2 °C with those obtained at zero magnetic field.

At each temperature the ^{13}C-{^{1}H} spectra yield a chemical shift, δ_i, for each of the 32 different ^{13}C nuclei in the isotropic phase, and for 30 in the liquid-crystal phases: the ^{13}C nuclei in the CN groups have large nuclear shielding constant anisotropies and as a consequence their peaks are broadened beyond detection in the orientationally ordered phases. Most of these resonances in the isotropic phase can be assigned by comparison with similar compounds, both monomers and dimers (for example, 5CB [22], 5OCB [23], and CB7CB [18]), and by two-dimensional (2D) NMR correlation experiments. The assignment of resonances in the nematic phases is less certain, mainly because it has not proved possible to perform a definitive NMR 2D correlation experiment such as INADEQUATE on samples in the LC phases for such large molecules.

III. COMPARISON OF THE ^{13}C-{^{1}H} SPECTRA IN THE ISOTROPIC PHASE AT 429 K WITH THAT OF A SAMPLE DISSOLVED IN $CDCl_3$ AT 298 K

The first step taken in order to assign the ^{13}C resonances in the spectra given by the liquid-crystal phases was to compare ^{13}C-{^{1}H} spectra of CB6OCB as a solution in $CDCl_3$, in which the peaks can be easily assigned by 2D NMR correlation experiments, with one obtained on CB6OCB in the isotropic phase above T_{NI}, as shown in Fig. 5.

The two spectra in Fig. 5 are clearly very similar, indicating that the assignment of the peaks to carbon positions is the same for both samples.

An expansion of the two spectra in the range 20–40 ppm is shown in Fig. 6, and for the range 105–165 ppm in Fig. 7.

The chemical shifts of the ^{13}C nuclei when the molecules are in isotropic phases depend on the molecular structure, and on the distribution of conformers generated by rotations about the bonds. The chemical shifts in the pure melt and in a solution in $CDCl_3$ have a mean square difference of 1.3 ppm from which it is concluded that the structure and conformational distributions are very similar in these isotropic phases.

IV. ASSIGNMENT OF THE ^{13}C RESONANCES IN CB6OCB IN THE NEMATIC PHASE, N_{U}

Figure 8 shows spectra of the aromatic carbons in the isotropic phase at 429 K, just above the N_{U} to I transition temperature of 426 K, and at 394 K in the nematic phase.

The assignment of the peaks from the nonprotonated, aromatic carbons on the *para* axes rested upon the following: (a) their intensities relative to those of protonated carbons; (b) they are expected, from quantum-chemical calculations, to have the largest shifts to higher frequency on changing from the isotropic to nematic phase; and (c) their shifts are assumed to be of the same order as in the isotropic phase, as are those from the protonated aromatic carbons.

The chemical shifts of the aliphatic carbons in the N_{U} phase cannot be assigned with certainty, except for that of carbon 24. The spectra from these aliphatic, spacer carbons in the two phases are compared in Fig. 9.

Note that the shift to lower frequency on going from the isotropic to nematic phases of the aliphatic carbons is consistent with density functional theory (DFT) calculations of the shielding anisotropies.

V. TEMPERATURE DEPENDENCES OF Δ_i, THE CHEMICAL SHIFT ANISOTROPIES FOR EACH CARBON SITE

The differences $\Delta_i = \delta_i(\mathrm{LC}) - \delta_i(\mathrm{I})$ for the ^{13}C nuclei in CB6OCB in its liquid-crystal and isotropic phases will be

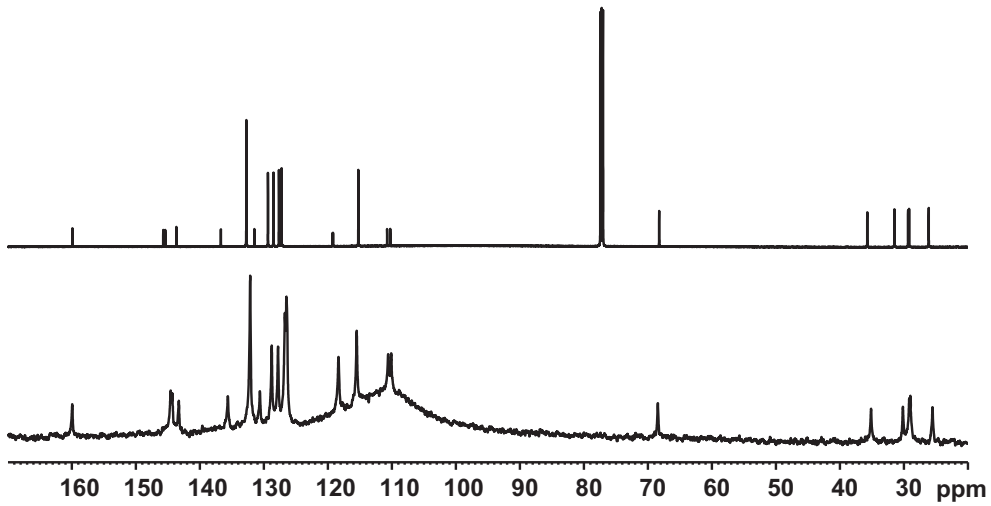

FIG. 5. The 150 MHz ^{13}C-{^{1}H} spectra of CB6OCB as a solution in $CDCl_3$ at 14 T (top) compared with a 125 MHz spectrum recorded at 11.7 T on the pure material in the isotropic phase at 429 K (bottom). The intense resonance at 77.23 ppm in the upper spectrum is from ^{13}C nuclei in the solvent, and the broad resonance at ∼110 ppm in the bottom spectrum is from ^{13}C in the spectrometer probe material. The two scales in ppm are the same, with the peaks at the highest frequencies made coincident. The spectrum in $CDCl_3$ solution was obtained by adding 1024 scans, acquired over a spectral window of 59.5 kHz, with an acquisition time of 1101.0 ms (65 536 complex points). The $\pi/2$ ^{13}C pulse was 14.45 μs and the recycle delay was 8.899 s. ^{1}H WALTZ-16 decoupling at 3.125 kHz was applied during acquisition. A weaker decoupling of about 0.95 kHz was applied during the recycle delay to increase the ^{13}C polarization by ^{1}H-^{13}C cross relaxation. The spectrum was processed with 65 536 complex points and using an exponential window function of 2.0 Hz. The spectrum in the isotropic phase is the result of acquiring 192 scans, each with a spectral window of 50.0 kHz, and an acquisition time of 102.4 ms (5120 complex points). The $\pi/2$ ^{13}C pulse was 5.0 μs and the recycle delay was 5.0 s. ^{1}H SPINAL64 decoupling at 25.0 kHz was applied during acquisition. The spectrum was processed with 65536 complex points and using an exponential window function of 2.0 Hz.

used to obtain values of S_{zz}(ArC) and S_{zz}(ArO), the order parameters for the z axes (*para* axes) of the cyanobiphenyl group attached to the aliphatic hexyl chain via either carbon or oxygen. The values of Δ_i are obtained by comparing the ^{13}C-{^{1}H} spectrum in the isotropic phase of CB6OCB above T_{NI} with spectra taken at temperatures throughout the two nematic phases. The temperature dependence of Δ_i for all the aromatic carbons has the same striking shape as that illustrated in Fig. 10 for C2 and C45, which are at analogous locations in the two cyanobiphenyl groups.

The transition from the N_U to N_{TB} phase produces a marked change in all the resonances, which is illustrated by the series of spectra for C2 and C45, shown in Fig. 11, obtained on cooling followed by heating. The small, discontinuous decrease in the values of Δ_i on entering the N_{TB} phase from the nematic at 383 K is consistent with the very small change in the transitional entropy ($\Delta S/R = 0.006$) measured for this weak, first-order transition [20].

The larger linewidths of the ^{13}C peaks in the N_{TB} phase could indicate a shorter value of T_2, the transverse spin

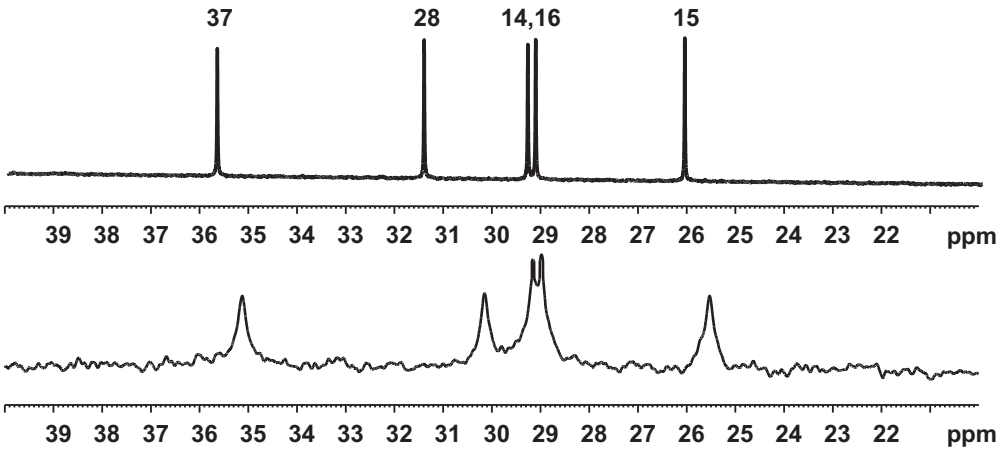

FIG. 6. Expansion of the 40−20 ppm region of the 150 MHz ^{13}C-{^{1}H} spectra of CB6OCB as a solution in $CDCl_3$ at 14 T and 298 K (top) compared with a 125 MHz spectrum recorded at 11.7 T on the pure material in the isotropic phase at 429 K (bottom). The peak labels in the $CDCl_3$ spectrum were obtained from 2D correlation experiments.

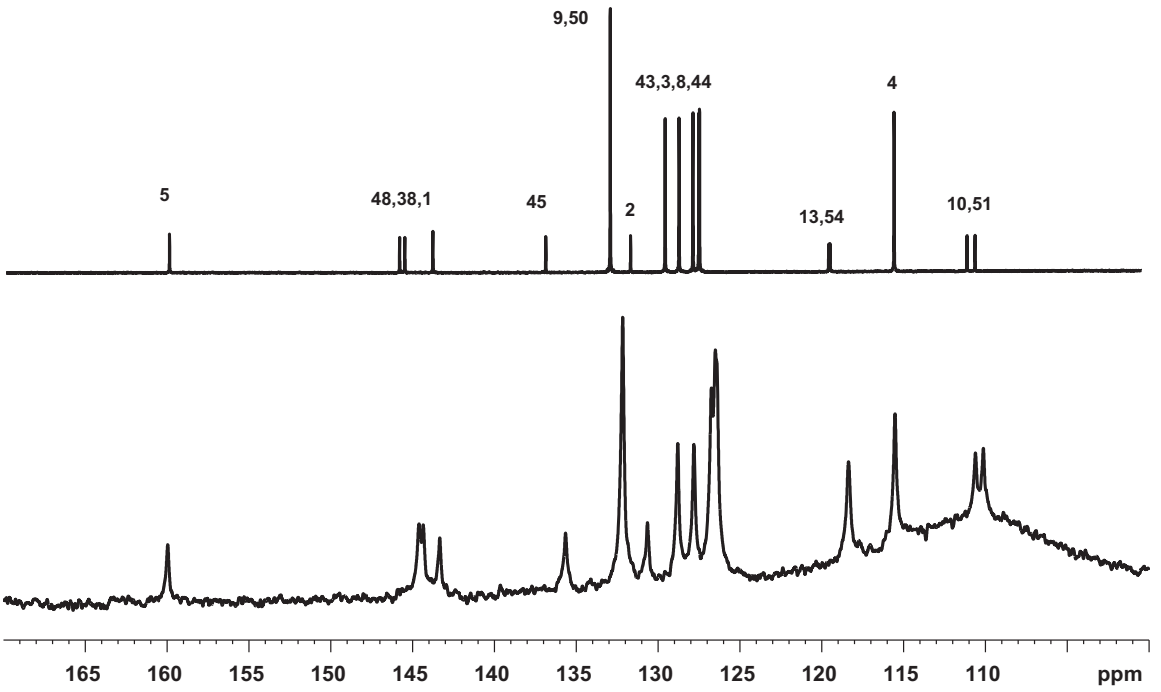

FIG. 7. Expansion of the 100–170 ppm region of the ^{13}C-{^{1}H} spectra of CB6OCB as a solution in $CDCl_3$ at 14 T and 298 K (top) compared with the same spectrum recorded at 11.7 T on the pure material in the isotropic phase at 429 K (bottom). The peak labels in the $CDCl_3$ spectrum were obtained from 2D correlation experiments.

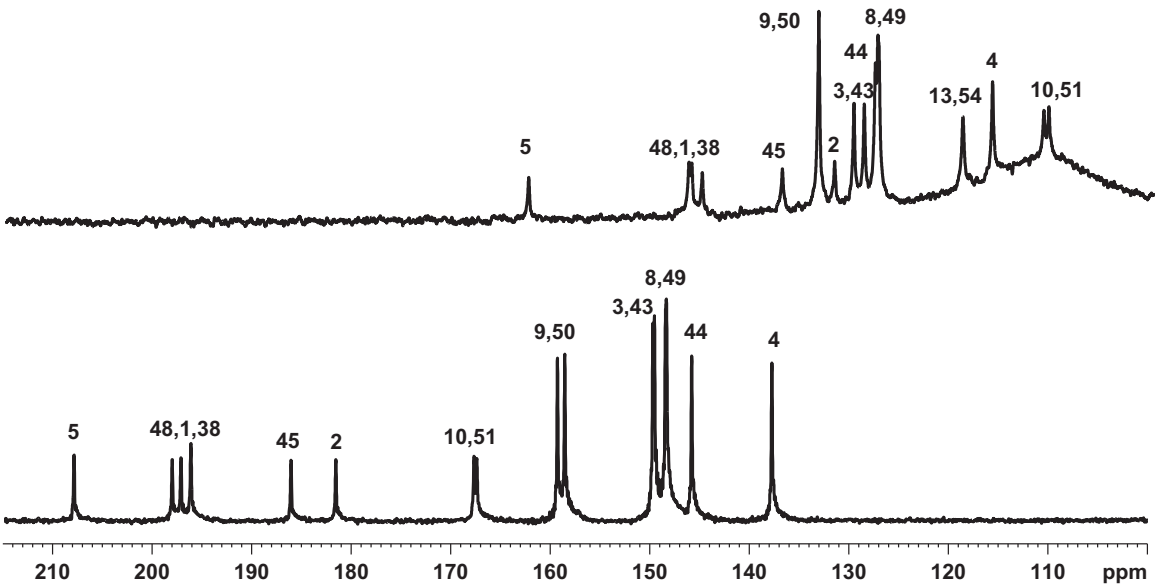

FIG. 8. The 125 MHz ^{13}C-{^{1}H} spectra of aromatic carbons in CB6OCB in the isotropic phase at 429 K (top) compared with the spectrum at a temperature in the nematic phase at 394 K (bottom). The isotropic phase spectrum was obtained by adding 192 scans, acquired over a spectral window of 50.0 kHz, with an acquisition time of 102.4 ms (5120 complex points). The $\pi/2$ ^{13}C pulse was 5.0 μs and the recycle delay was 5.0 s. ^{1}H SPINAL64 decoupling at 25.0 kHz was applied during acquisition. The spectrum was processed with 65536 complex points and using an exponential window function of 2.0 Hz. The spectrum in the nematic phase (394 K) was acquired with a ^{1}H-^{13}C cross-polarization (CP) sequence adding up 96 scans, each with a spectral window of 31.25 kHz, and an acquisition time of 55.9 ms (1747 complex points). The $\pi/2$ ^{1}H pulse was 5.0 μs, the CP contact time was 3.0 ms and the recycle delay was 5.0 s. The CP power levels were 38.3 kHz for ^{1}H and 31.5 kHz for ^{13}C. Proton decoupling was applied using SPINAL64 with a rf field strength of 53.2 kHz during acquisition. The spectrum was processed with 16 384 complex points and using an exponential window function of 10.0 Hz.

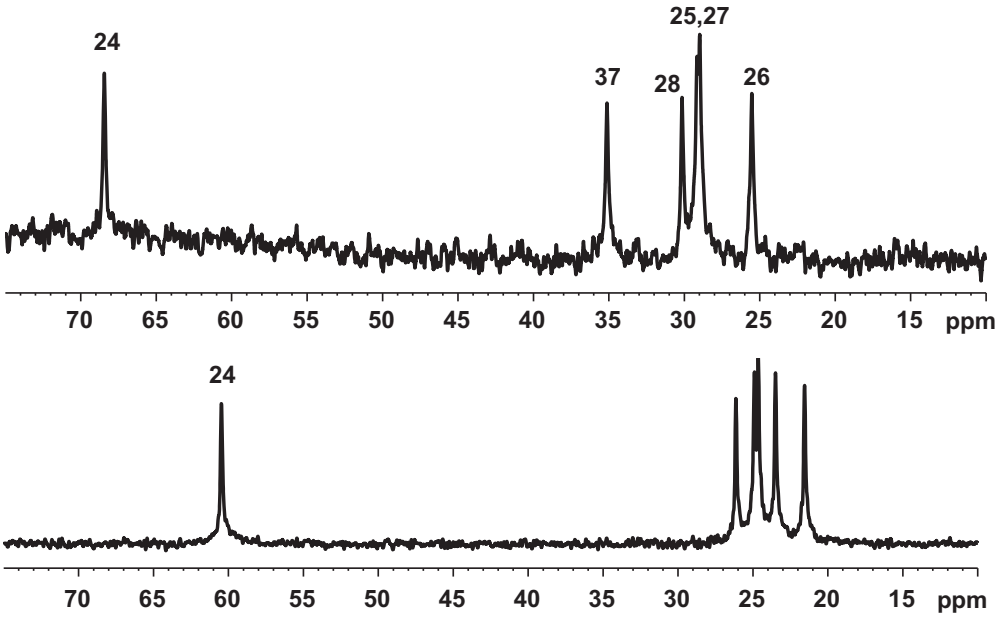

FIG. 9. The 150 MHz ^{13}C-{^{1}H} spectra of aliphatic carbons in CB6OCB in the isotropic phase at 429 K (top) at 14 T compared with the spectrum recorded at 125 MHz and at 11.7 T, and at a temperature in the nematic phase of 394 K (bottom).

relaxation rate, caused by a slowing of whole-molecule rotation, or the presence of a distribution in the alignment of the local directors relative to the applied magnetic field. It is of interest that the disordered twist-bend nematic phase obtained from the frozen sample was aligned by the magnetic field (11.7 T) of the NMR spectrometer within a maximum time of 20 min. The alignment of the twist-bend nematic phase of CB7CB with a weaker magnetic field of 7.05 T has been studied [6,24], and in this case the director, the helix axis, was initially orthogonal to the magnetic field and not randomly aligned as for CB6OCB. The sample temperature was also 12 K below the N_{TB}-N_U transition and it was found that after about 5 min, although much of the sample had been aligned parallel to B, there were still significant defects with domains perpendicular to B.

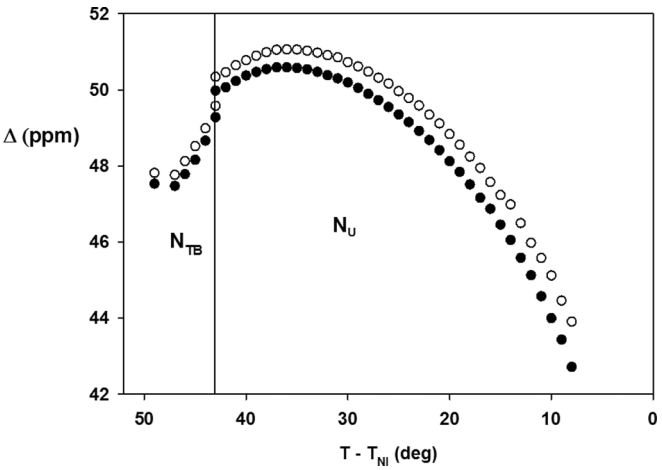

FIG. 10. Chemical shift anisotropies for C2 (○) and C45 (●) in the nematic and twist-bend nematic phases of CB6OCB as a function of temperature.

The N_U-N_{TB} phase transition was observed to occur at 382 K outside the magnetic field [20]. Measurement of the temperature of the sample in these NMR experiments has a precision of about 1°C–2 °C, and therefore there is no evidence for an effect of the 11.7-T magnetic field on this phase transition. Thus these spectra show that the sample is entirely in the N_U phase at 382 K, and entirely in the N_{TB} at 384 K, while at 383 K both the N_U and N_{TB} phases are present. This small biphasic region could originate from the presence of small amounts of impurities, but might also reflect the presence of a temperature gradient over the sample. A striking feature of the spectrum in the biphasic region is that the peaks for the N_U phase sharpen from ∼35 to ∼20 Hz.

The spectra in Fig. 11 also show that the magnetic field is producing the same uniformity of alignment of the phase director (the helix axis) on heating from the solid or cooling from the N_U phase.

VI. QUANTIFYING THE ORIENTATIONAL ORDER OF THE CYANOBIPHENYL GROUPS

The anisotropic chemical shifts, Δ_i, are related to order parameters $S_{\alpha\beta}$ for axes xyz (Fig. 12) fixed in the hexylated or hexyloxylated substituted ring by

$$\begin{aligned}\Delta_i = {} & \tfrac{2}{3}S_{zz}\left[\sigma_{izz} - \tfrac{1}{2}(\sigma_{ixx} + \sigma_{iyy})\right] \\ & + \tfrac{1}{3}(S_{xx} - S_{yy})(\sigma_{ixx} - \sigma_{iyy}) \\ & + 4[S_{xy}\sigma_{ixy} + S_{xz}\sigma_{ixz} + S_{yz}\sigma_{iyz}]/3, \end{aligned} \quad (1)$$

where σ_{izz}, etc., are elements of the shielding tensor for atom i. Studies on other mesogens containing these groups [15,27–32] suggest that to a good approximation only the term involving S_{zz} is of appreciable magnitude for carbon atoms, which are on the z axis, and so Δ_i and S_{zz} for these sites are linearly related:

$$\Delta_i = A_i S_{zz}. \quad (2)$$

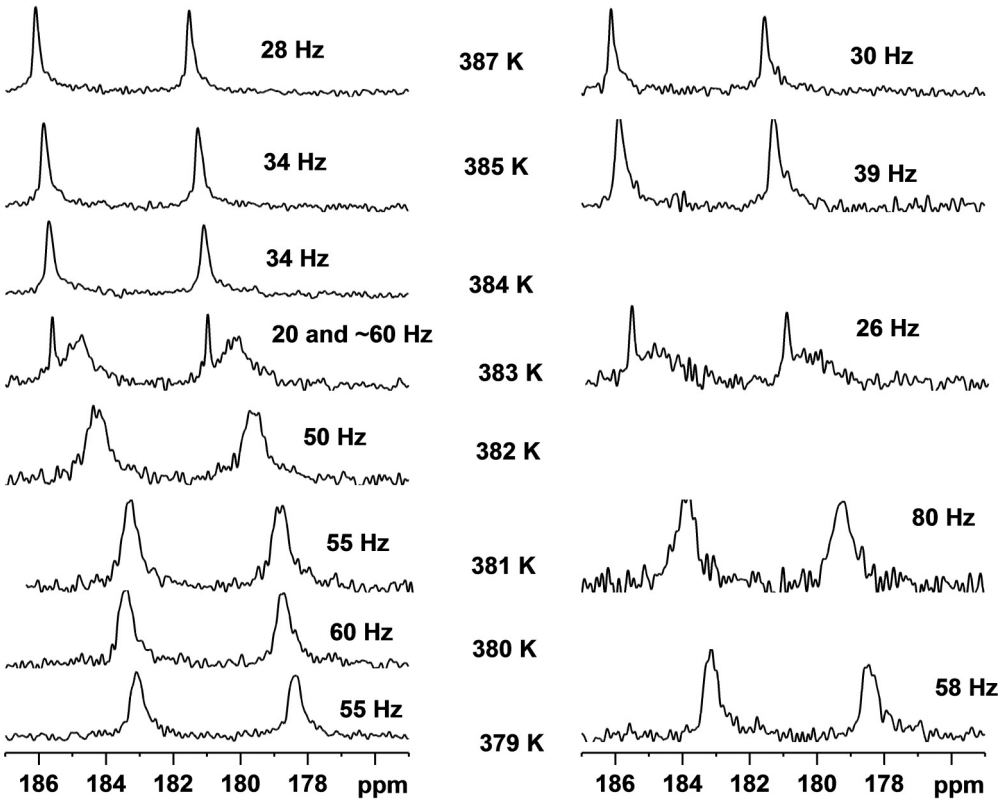

FIG. 11. The 125 MHz ^{13}C-{^{1}H} spectra of carbons 2 and 45 in CB6OCB as the temperature is lowered from 387 K in the N_U phase (left column). The spectrum at 383 K shows peaks from both N_U (sharp) and N_{TB} (broad) phases. The sample froze at ~376 K, and was then heated from the solid back to 387 K and left for 20 min at each temperature before obtaining the spectra shown in the right column. The linewidths are shown alongside each set of peaks for each temperature.

To use this simple relationship to obtain the temperature variation of S_{zz} it is necessary to obtain a value for the constant A_i for at least one carbon site on each *para* axis in each biphenyl fragment at one temperature. This has been achieved by obtaining proton-encoded, ^{13}C-decoupled (PELF) spectra [33,34] by the method illustrated in Fig. 13.

PELF spectra were obtained on a sample in the N_U phase at 394 K (see Figs. 14 and 15), and in the same phase at 390 K, and 377 K that is the N_{TB} phase.

The sections parallel to the *F1* axis, corresponding to the time variable t_1 in Fig. 13, at each chemical shift δ_i in the PELF spectra yield the magnitudes $|kT_{i,j}| = k(J_{i,j} + 2D_{i,j})|$ of the scaled total spin-spin couplings, where the scaling factor k is dependent on the homonuclear refocusing pulse sequence, and for the sequence used here it has been calibrated to be 0.47 ± 0.02 [22]. The scalar spin-spin couplings were taken to have the values measured for isotropic-phase samples of 5CB [22] and 5OCB [23].

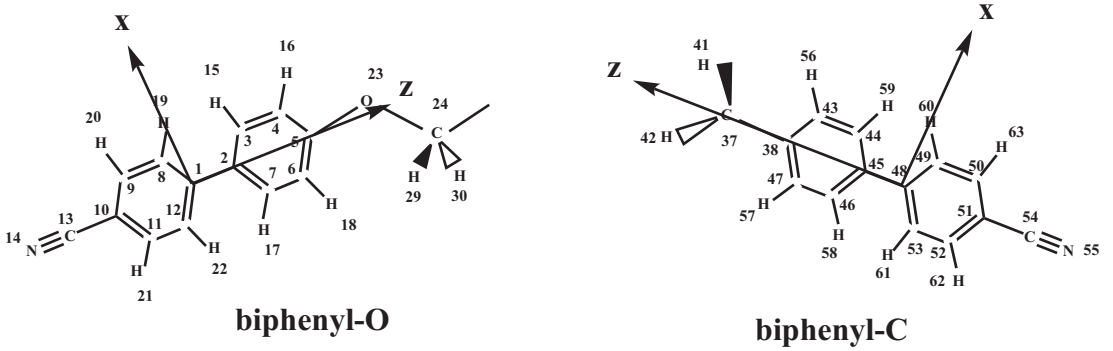

FIG. 12. Reference axes for the cyanobiphenyl groups in CB6OCB. For the hexyloxylated ring (biphenyl-O) the z axis is parallel to the C1-C2 bond, and x is in the plane defined by C1, C2, C3. Note that z makes an angle of ~4° with the C-O bond [25–27]. For the hexylated ring (biphenyl-C) z is along the C48-C45 bond, and x is in the plane C48, C45, C44. The bond C37-C38 is parallel to z.

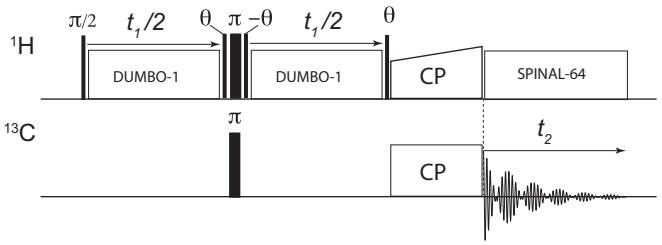

FIG. 13. The PELF-NMR experiment.

VII. BIPHENYL GROUP ORDER PARAMETERS

The residual dipolar couplings (RDCs) between pairs of nuclei, within each phenyl ring in the biphenyl groups, $D_{i,j}$, are related to local order parameters relative to the axes shown in Fig. 12 by

$$D_{i,j} = -\frac{K_{i,j}}{r_{i,j}^3}[S_{zz}(3\cos^2\theta_{ijz} - 1) + (S_{xx} - S_{yy})(\cos^2\theta_{ijx} - \cos^2\theta_{ijy}) + 4S_{xy}\cos\theta_{ijx}\cos\theta_{ijy} + 4S_{xz}\cos\theta_{ijx}\cos\theta_{ijz} + 4S_{yz}\cos\theta_{ijy}\cos\theta_{ijz}], \quad (3)$$

with

$$K_{i,j} = \mu_0\gamma_i\gamma_j h/32\pi^3. \quad (4)$$

For ^{13}C and ^{1}H nuclei separated by 1 Å the value of $(K_{i,j}/r_{i,j}^3)$ is 15094.27 Hz.

Consider first the biphenyl-C group in Fig. 12. The cyanylated ring rotates about the C45-C48 bond and the hexyl chain about C38-C37, while to a good approximation, the structure of the phenyl ring in which the *xyz* axes are fixed is unchanged by this internal motion. As a consequence the RDCs between nuclei within this fixed ring do not depend on the terms involving S_{xy}, S_{xz}, or S_{yz}, even though these order parameters are not zero [28]. The magnitudes of $T_{44,59} = T_{46,58}$ and $T_{44,56} = T_{46,57}$ are extracted from the PELF spectrum for the aromatic carbons (see Fig. 14), but not their signs. To determine their signs the values of these two RDCs were calculated by assuming reasonable values of the two order

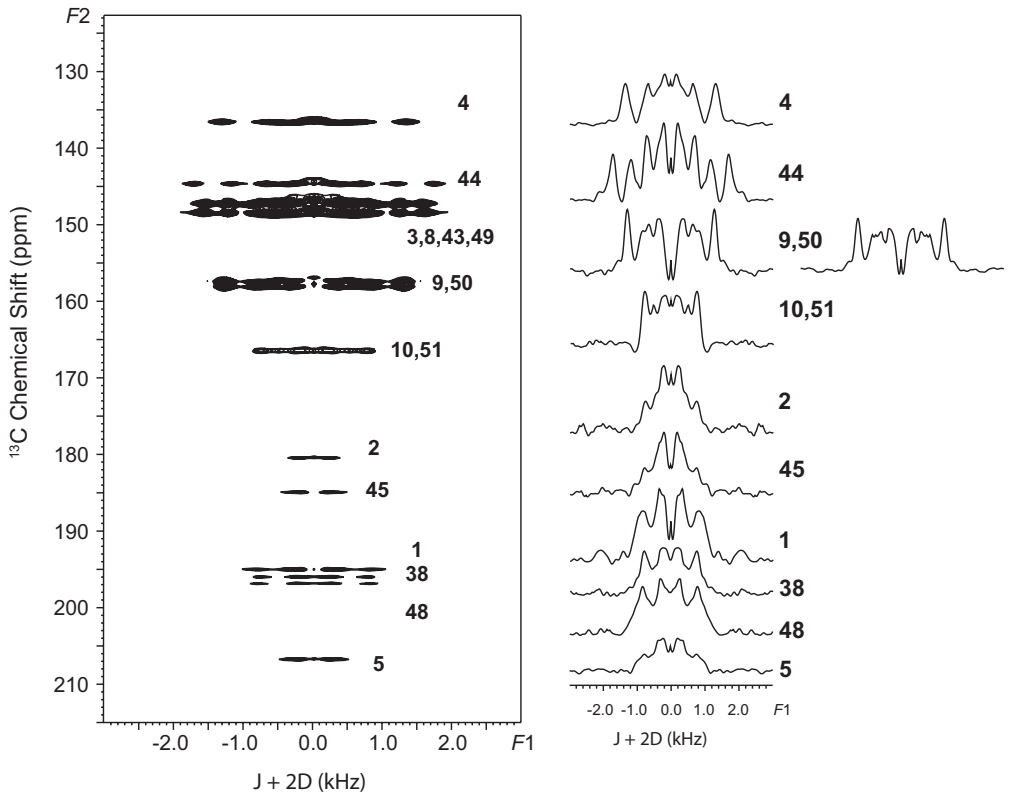

FIG. 14. ^{13}C-^{1}H PELF-NMR spectrum at 11.7 T of the aromatic carbons in the nematic phase of CB6OCB at 394 K. The $F1$ axis has been adjusted to allow for the scaling factor of 0.47 introduced by the homonuclear refocusing sequence [22]. The spectrum was recorded at 11.7 T (125 MHz ^{13}C Larmor frequency) on an Avance III Bruker spectrometer using a double resonance probe (static horizontal probe, 4-mm sample tube). The ^{1}H and ^{13}C$\pi/2$ pulses were calibrated to be 2.5 and 5.0 μs each; DUMBO-1_{22} decoupling was applied at a rf field strength of 50 kHz (DUMBO cycle time of 60 μs). The contact time for the polarization transfer step was 2.5 ms using a 50%–100 % ramp of power on the ^{1}H channel (with 36.8 kHz of maximum rf field strength) and a constant rf power of 23.7 kHz on the ^{13}C channel. ^{1}H SPINAL-64 decoupling was applied during acquisition with a rf field strength of 50 kHz. Up to 144 scans per increment were collected and added together, with 192 t_1 increments. The total acquisition times were 34.9 ms for the direct dimension and 12.3 ms for the $F1$ dimension. The recycle delay was 5.0 s with a total experiment time of 15 h.

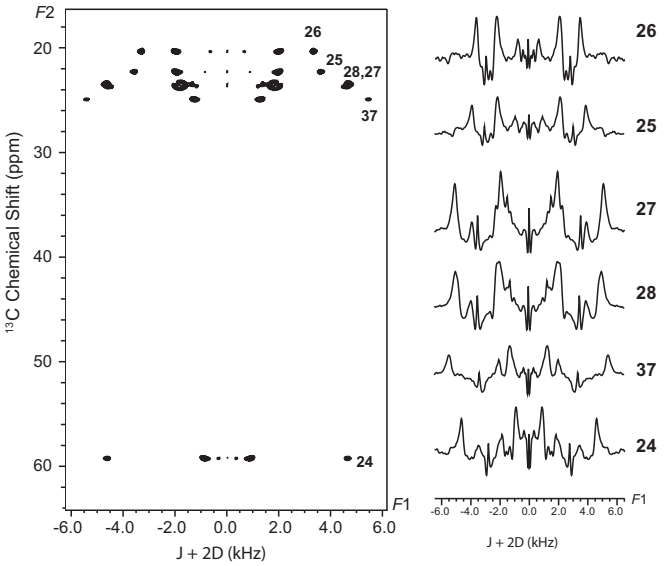

FIG. 15. ^{13}C-^{1}H PELF-NMR spectrum at 11.7 T of the aliphatic carbons in CB6OCB at 394 K. The projections onto the *F2* axis are at the positions of the ^{13}C chemical shifts, with the assignment discussed in the text. The experimental parameters are reported in the caption of Fig. 14.

parameters, namely, $S_{zz} = 0.5$ and $S_{xx} - S_{yy} = 0$. To make these calculations it is also necessary to assume values for the coordinates of the atoms in the ring, and these were taken to be those found by a quantum-mechanical calculation of the structure of CB6OCB in its minimum-energy conformation. The details of this DFT calculation, and the results are given in the Supplemental Material [35].

Having determined the magnitudes and signs of $D_{43,56} = D_{47,57} = 1653$ Hz, and $D_{43,59} = D_{47,58} = -1156$ Hz these were used to obtain S_{zz} and $S_{xx} - S_{yy}$ for the axes shown in Fig. 12 for the biphenyl-C ring, giving $S_{zz} = 0.526$ and $S_{xx} - S_{yy} = 0.053$ for 394 K. The errors on these values have contributions from the errors on the RDCs ($\sim \pm 1\%$) and the geometry used. The latter errors were estimated by repeating the calculation but using a model geometry having the benzene rings as regular hexagons with C-C bond lengths of 1.400 Å and C-H of 1.087 Å. With this geometry $S_{zz} = 0.540$ and $S_{xx} - S_{yy} = -0.007$.

Calculating the local order parameters for phenyl groups within the biphenyl-O ring is made more complicated by the significant change in geometry [23,25–27] as the hexyloxy chain rotates about the z axis ($\theta_{23,5,4} = 115^\circ$ interchanges with $\theta_{23,5,6} = 125^\circ$ with smaller but still significant changes in neighboring angles). The geometry of the other, CN-substituted ring is barely affected by this nonrigid rotation and so the local order parameters for the biphenyl-O group were calculated by fixing *xyz* in the CN phenyl ring and calculating local order parameters from $D_{9,20} = D_{11,21} = 662$ Hz, and $D_{9,19} = D_{11,22} = -1267$ Hz. This gives $S_{zz} = 0.559$ and $S_{xx} - S_{yy} = 0.110$, and for the model geometry $S_{zz} = 0.575$ and $S_{xx} - S_{yy} = 0.117$. The z axis is common to both rings in a biphenyl group, but the x and y axes fixed in each ring are not parallel to one another, their relative orientations depending on the inter-ring angle, ϕ_{ring}, in the mimimum-energy conformation. The DFT calculations give $\phi_{\text{ring}} = 37.9^\circ$ for the biphenyl-O ring and 38.8° for the biphenyl-C when the rest of the molecule is in the minimum-energy conformer. These values compare with ∼30° for 5CB [29] and 6OCB [30] when in the nematic phase.

TABLE I. Order parameters S_{zz} and $S_{xx} - S_{yy}$ for axes *xyz* fixed in either the biphenyl-O or biphenyl-C rings of CB6OCB when the sample is in the N_{U} phase at 394 and 390 K, and in the N_{TB} phase at 377 K.

T (K)	Phase		S_{zz}	$S_{xx} - S_{yy}$
394	N_{U}	O-ring	0.559	0.110
		C-ring	0.526	0.053
390	N_{U}	O-ring	0.571	0.083
		C-ring	0.569	0.077
377	N_{TB}	O-ring	0.508	0.090
		C-ring	0.521	0.088

Calculations of the local order parameters for the phenyl rings were also made using values of the RDCs obtained at 390 and 377 K, and they are given in Table I.

The errors in measuring the dipolar couplings are about 1%, leading to errors in the order parameters from this source of about 1% in S_{zz} and 2% in $S_{xx} - S_{yy}$. The relative values of the order parameters given in Table I have this level of precision from experimental errors, but there are also systematic errors in the values obtained for the order parameters, such as the use of the geometry obtained by the DFT calculations, and the neglect of the effect of vibrational motion, which are impossible to quantify precisely, but which may be as much as ∼5%.

Values of A_i in Eq. (2) were obtained for carbon C2 ($A_2 = 90.424$ ppm) in the O- and C45 ($A_{45} = 92.106$ ppm) in the C-biphenyl groups by using the values of Δ_i and S_{zz} at 394 K. This enabled values of S_{zz} for the biphenyl-O and biphenyl-C rings to be calculated at all other temperatures, and these are

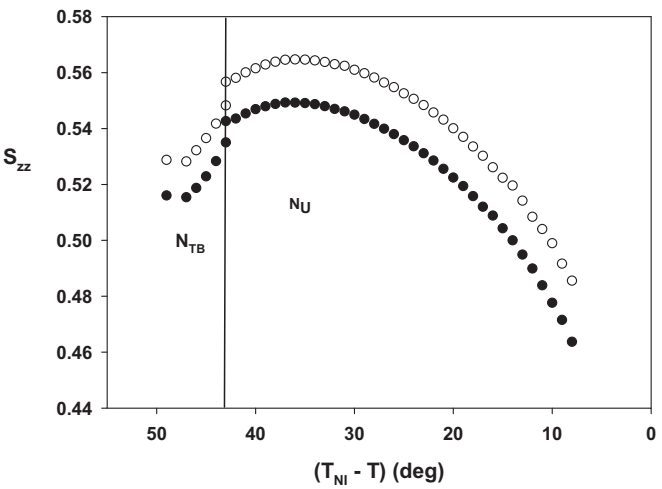

FIG. 16. Temperature dependence of S_{zz} for the *para* axes in the O-ring (○) and C-ring (●) of CB6OCB determined from the chemical shift anisotropies of the carbons C2 and C45.

shown in Fig. 16. The z axes of the two biphenyl groups are not coparallel, and their local order parameters are not, therefore, expected to be equal in magnitude.

The temperature profiles of S_{zz} obtained for CB6OCB are similar in shape to that measured [15] for the symmetric dimer DTC5C9, (see Fig. 4) which also exhibits $N_{\rm U}$ and $N_{\rm TB}$ phases. For both compounds $S_{zz}(T)$ has a maximum in the $N_{\rm U}$ phase: For DTC5C9 this occurs at ∼28 K below the $N_{\rm U}$-I transition and ∼9 K above the transition to the $N_{\rm TB}$ phase, while for CB6OCB the maximum is ∼35 K below T_{NI} and ∼8 K above $T_{N_{\rm TB}N}$. In contrast, the temperature range for the nematic phase of CB7CB is much shorter (∼13 K) than either DTC5C9 or CB6OCB, and $S_{zz}(T)$ is like those of conventional nematic liquid crystals reaching its largest value at the transition to the $N_{\rm TB}$ phase.

The order parameter, S_{zz}, of the biphenyl groups is certainly not expected, from either experiment or theory, to exhibit a maximum with changing temperature. However, the biaxial order parameter, $S_{xx} - S_{yy}$, is found to pass through a maximum when the molecular biaxiality is sufficiently large. Examples of this include the deuterated probe, quinizarin-d_6, dissolved in the liquid-crystal dimers CBO9OCB and CBO10OCB as well as the monomers 6OCB and 7OCB [36] and another probe, anthracene-d_{10}, dissolved in CB7CB and CBO5OCB [37]. Such behavior is in accord with a molecular field theory of uniaxial nematics formed from biaxial molecules [38]. This interpretation of the maximum in $S_{zz}(T)$ cannot be used to account for the maximum found for CB6OCB since the order parameters have been carefully measured from chemical shift anisotropies of the ^{13}C nuclei on the *para* axes, which have a negligible contribution from the term in Eq. (1) dependent on the biaxial order parameter $(S_{xx} - S_{yy})$. The maximum might result from a change in the molecular shape caused by a conformational variation in the spacer topology. However, as is shown in Fig. 23 (see later), the similarity in the residual dipolar couplings, $^1D_{\rm CH}$, in the spacer measured in the $N_{\rm U}$ (394 K) and the $N_{\rm TB}$ (377 K) phases suggests that such a significant difference in the conformational distribution does not exist.

Having eliminated possible explanations for the maximum we now turn in the following section to that proposed for the dimer DTC5C9 [15], namely, that the director in the $N_{\rm U}$ phase tilts with decreasing temperature away from the magnetic field of the spectrometer.

VIII. ESTIMATE OF THE TILT ANGLE IN BOTH NEMATIC PHASES

The existence of a maximum in $S_{zz}(T)$ was attributed for DTC5C9 to a tilting of the directors in the $N_{\rm U}$ phase from being aligned along the magnetic field direction to being tilted through a temperature-dependent angle, $\theta_0(T)$. This was found to increase almost continuously as the sample entered the $N_{\rm TB}$ phase. The values of $\theta_0(T)$ were obtained by comparing the order parameters $S_{zz}(T)$ obtained by experiment with values predicted by assuming that this order parameter should follow a Haller curve [39]. Indeed, the experimental temperature dependence of the major order parameter, $S_{aa}(\Delta T)$, for many "classic," rodlike nematic liquid crystals, is found to follow the equation

$$S_{aa}(\Delta T) = S_{aa}(0)(\Delta T/T_{NI})^{\gamma}, \tag{5}$$

where $\Delta T = T_{NI} - T$, and $S_{aa}(0)$ is the value of S_{aa} when the sample is at 0 K. For a rigid, axially symmetric nematic liquid crystal the value of $S_{aa}(0) = 1$, but for real nematic liquid crystals it is treated as a fitting parameter, as is the exponent γ. Equation (5) predicts a zero value for S_{aa} at T_{NI} rather than the finite value found experimentally. This anomaly of the Haller function can be allowed for by replacing T_{NI} by T_{NI^*} which is treated as an added variable when values of S_{aa} can be obtained up to T_{NI}. In the present case of CB6OCB values of $S_{aa}(\Delta T)$ could not be obtained for $T_{NI} - T < 6$ K, and consequently the unmodified value of T_{NI} was retained in Eq. (5). Note that for "classic" nematic liquid crystals with either approximately linear, or with bent shapes [31,32], $S_{aa}(\Delta T)$ is found to increase as the temperature decreases from T_{NI} and reaches its largest value at the lowest temperature for the existence of the phase. The observed values of S_{zz} for the two biphenyl groups in CB6OCB deviate from the case of a classic nematic in having a maximum value in the $N_{\rm U}$ phase before reaching the temperature of transition, $T_{N_{\rm TB}N_{\rm U}}$, to the twist-bend phase. This behavior is explained by assuming that at the highest temperatures in the $N_{\rm U}$ phase the values of $S_{zz}(\Delta T)$ should follow a Haller function, but that a tilt, ϕ, of the liquid-crystal director away from the direction of the applied magnetic field begins to develop at lower temperatures, but before the maximum of S_{zz} in the nematic phase. The parameters $S_{zz}(0) = S_{aa}(0)$ and γ in Eq. (5) were obtained as 0.783 ± 0.002 and 0.132 ± 0.001 respectively, compared to 0.82 and 0.17 for DTC5C9, which has a similar bent shape, by fitting to 11 values of $S_{zz}(T)$ at temperatures in the range 418–407 K, which were then used to predict values of S_{zz} throughout the rest of the $N_{\rm U}$ and into the $N_{\rm TB}$ phase. Figure 17 shows the result for the values of S_{zz} obtained from the shift anisotropies of C45.

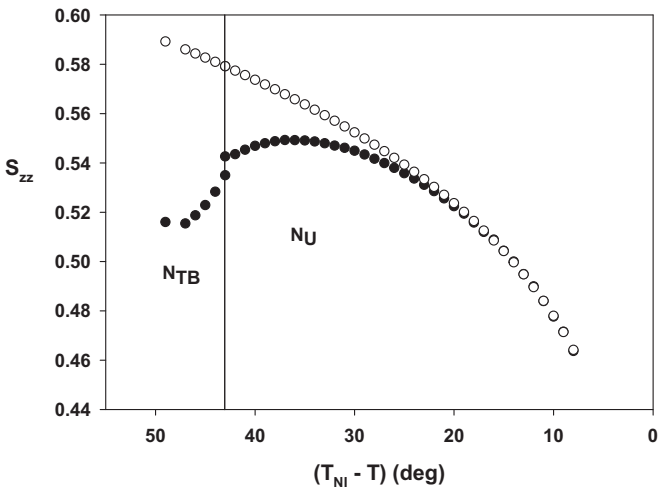

FIG. 17. Comparison of $S_{zz}(T)$ determined from the shift anisotropy of C45 (●) in biphenyl-C with values (○) calculated for the Haller function of Eq. (5) with $S_{aa}(0) = 0.783$ and $\gamma = 0.132$.

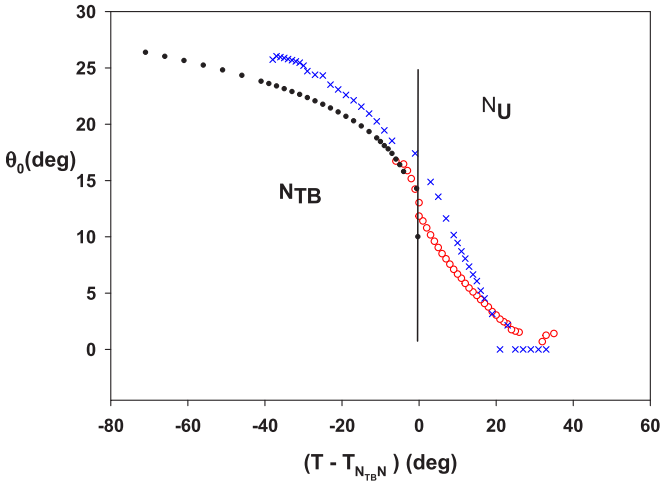

FIG. 18. The temperature dependence of θ_0, the tilt of the director away from the applied magnetic field, determined from S_{zz} for the C-ring in CB6OCB (○) compared with values obtained by a similar method for DTC5C9 (×) [15], and from the deuterium quadrupolar splittings in CB7CB-d_4 (●) (taken from [40]).

The observed order parameters, $S_{zz}(T,\text{obs})$, in both phases, are related to those predicted by the Haller function, $S_{zz}(T,\text{pred})$ by

$$S_{zz}(T,\text{obs}) = S_{zz}(T,\text{pred})(3\cos^2\theta_0 - 1)/2. \quad (6)$$

The values of the tilt angle, θ_0, obtained at each temperature are shown in Fig. 18.

The reasons for the finite values of θ_0 in the N_U phase for CB6OCB and DTC5C9 are not obvious. The discontinuous change by $\sim 1^\circ$ on entering the N_{TB} phase of CB6OCB, expected for a weak first-order transition, can be attributed to the proposed formation of a helical arrangement of local directors, with the helix axis acting as the phase director and aligning along the applied magnetic field direction, as shown in Fig. 1. In this model for the N_{TB} phase θ_0 is expected, as observed, to increase on decreasing temperature.

The conical angle θ_0 has been measured for other nematic liquid crystals forming the twist-bend nematic phase. The first compound to be identified as exhibiting this intriguing phase is the liquid crystal dimer CB7CB [6]. It is not surprising therefore that so far most studies of the conical angle have been made for this system. It is also of significance that the nematic range for CB7CB is relatively short, just 13 °C, whereas that for CB6OCB is 44 °C and for DTC5C9 is 37°C. One consequence of this is that the N_{TB}-N_U transition is stronger for CB7CB than for CB6OCB or DTC5C9; this difference is in keeping with the analogy between the twist-bend nematic and the smectic-A phase [41,42]. It should also be noted that for CB7CB with its stronger phase transition the orientational order in the nematic phase, measured with ^{2}H and ^{129}Xe NMR spectroscopy [6,40], continues to increase until the N_{TB} phase is reached. At this point there is a small but significant increase in the order followed by a continuing weak increase in this through the twist-bend nematic phase with decreasing temperature. Analysis of this dependence for ^{129}Xe and ^{2}H in deuterated CB7CB allows the conical angle to be estimated [40]. There is a jump of about 10° at the transition and then growth in the conical angle which reaches 25° when the shifted temperature $(T_{N_{TB}N} - T)$ reaches 60 K. A qualitatively different analysis of the quadrupolar splitting for the monomer 8CB-d_2 doped into CB7CB shows a smaller jump in the conical angle of 3° at the phase transition but a comparable value of about 22° at the same shifted temperature of 60 K [43]. The difference with previous results is perhaps to be expected because a solute molecule is being used although with ^{129}Xe similar results are obtained [40]. A different technique has been used to estimate the cone angle, again for CB7CB, based on measurements of the birefringence in both the nematic and twist-bend nematic phase [44]. This study reveals essentially the same jump of 10° at the transition although the angle then grows rapidly until, just before the shifted temperature of 60 K, it reaches a value of 36°. It is possible that the technique employed has an influence on the experimental result which differs in comparison with the results obtained using NMR spectroscopy.

Recently a study of the lower homologue DTC5C7 with a heptane spacer has been published [45] which is of relevance to our study. The nematic range of this liquid-crystal dimer is 31.1 K, just ∼6 K less than that for DTC5C9. The measurements of the birefringence indicates that the orientational order in the N_U phase passes through a weak maximum prior to what is described as an N_X phase although having similar properties to an N_{TB} phase. Analysis of the temperature dependence, following Meyer *et al.* [42], suggests that the conical angle grows steeply on entering the N_X phase and reaches a plateau of $\sim 9^\circ$ before growing again to $\sim 12^\circ$ at 9 K into the phase. It is of interest to note that there is a change in the gradient of the dielectric permittivity in the N_U phase at about 413 K, the temperature above which the Haller function is found to fit the temperature variation of the birefringence. In contrast this function is found to fit the diamagnetic anisotropy well over the entire range of the N_U phase.

IX. CONFORMATIONAL DISTRIBUTION FOR THE HEXYL CHAIN

The two biphenyl groups are connected by a -O(CH$_2$)$_6$- group which is flexible by virtue of rotation about each of the O-C and C-C bonds, as shown in Fig. 19 .

In the solid phase the molecule probably exists in a single, rigid, minimum-energy form, but in the gas phase, and in each liquid phase it is expected that there will be phase-dependent distributions of conformations, $P_{\text{gas}}(\{\phi(k)\})$, $P_{\text{iso}}(\{\phi(k)\})$, $P_{N_U}(\{\phi(k)\})$, and $P_{N_{TB}}(\{\phi(k)\})$, and each of these will almost certainly be different. For each distribution, $\{\phi(k)\}$ is a set of continuous functions describing the bond rotations. The probability distributions strongly influence the stability of each phase, as well as the phase transition temperatures, and so the characterization of the distributions for the condensed fluid phases is essential for a full understanding of these properties. Early attempts for the predictions of these include the pitch, conical angle, order parameter, and elastic constants [46].

The conformational distributions may also be important in understanding why the N_{TB} phase is enantiomorphic. Thus the rotations about each of the bonds in CB6OCB in a single, isolated molecule generate conformational states which have either a plane of mirror symmetry and are therefore achiral, or

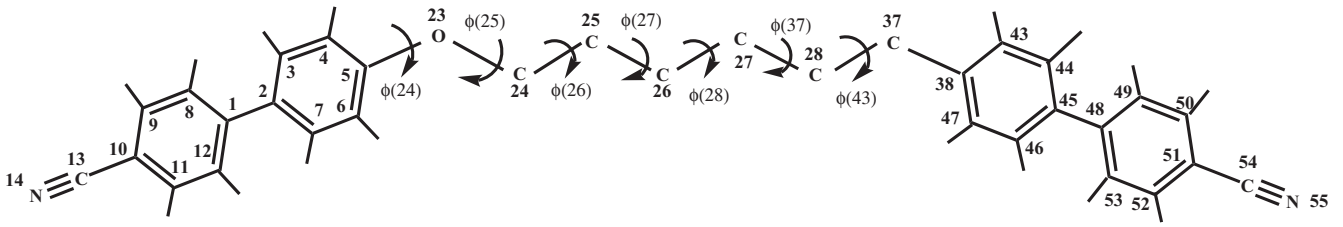

FIG. 19. Torsional rotations about bonds in the -O(CH_2)$_6$- flexible spacer in CB6OCB.

exist in pairs of equal probability with opposite chirality, so that the molecules are achiral when averaged over all rotational conformations. It has been suggested that in the N_{TB} phase the individual molecules may become chiral because of a loss of the mirror symmetry for rotation about one or more bonds, and that there is separation into domains in each of which there is a bias towards one of the two enantiomeric molecular forms [16,17]. An alternative explanation is that individual molecules remain achiral, but they aggregate into chiral forms, such as the helicoidal structure of local directors sketched in Fig. 1. The helices are either *P* or *M* in their sense of rotation, and in the absence of a chiral constraint, such as a dissolved, pure enantiomer [47], the sample will form a conglomerate of domains of opposite handedness.

X. BOND ROTATIONS IN AN ISOLATED MOLECULE OF CB6OCB

The torsional potential governing each bond rotation will be a continuous function V $[\phi(k)]$ of a dihedral angle $\phi(k)$. Thus a rotation about the bond C(i)-C(j) in the fragment C(r)-C(i)-C(j)-C(k) is described by the dihedral angle $\phi(k)$ made by the bond C(j)-C(k) relative to the plane described by atoms C(r), C(i), and C(j). The rotation described by $\phi(24)$ is governed by the potential,

$$V[\phi(24)] = V_{24}[1 - \cos 2\phi(24)], \qquad (7)$$

which has a single maximum at 90° and equal minima at 0° and 180°. The minimum-energy conformers are shown in Fig. 20.

As noted earlier the bond angle θ (23,5,4) changes from being 124° in the conformer with $\phi(24) = 0°$, to 116° in the other, $\phi(24) = 180°$, minimum-energy form. This means that rotation about the z axis involves geometrical changes, and is not the same as rotation about the C5-O23 bond.

The rotation about the C28-C37 bond is also predicted to be between two minimum-energy forms, but now with minima at 90° and 270° and a maximum at 0°. The other C-C bond rotations in the chain are each between three energy minima: two energy equivalent conformers at $\phi(k) \approx \pm 64°$

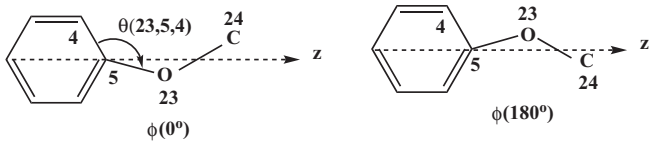

FIG. 20. The two minimum-energy structures for rotation through the dihedral angle $\phi(24)$ in CB6OCB.

(*gauche* forms), and a unique form at $\phi(k) = 180°$ (*trans*). The rotation about O23-C24 is also between two equivalent *gauche* forms, but now having $\phi(k) \approx \pm 83°$ and a *trans* form at 180°, as predicted by the DFT B3LYP/6-311G** calculations on an isolated, single molecule of CB6OCB (see Supplemental Material [35]). These calculations predict the energy differences between the minimum-energy forms given in Table II.

The minimum-energy conformation of the alkyl chains in alkylcyanobiphenyl liquid crystals (*n*CB) are all assumed to have each C(r)-C(i)-C(j)-C(k) fragment in the *trans* configuration, although this has been confirmed experimentally only for 5CB [29]. An experimental study on the nematic liquid crystal 6OCB found that the hexyloxy chain fragment O-C(r)-C(i)-C(j)-C(k) has $\phi(k) \approx \pm 64°$, with all other fragments in the *trans* configuration in the two equivalent minimum-energy forms [30] in both the pretransitional region of the isotropic phase, and the nematic phase. This result compares with calculations of the minimum-energy conformations by DFT on isolated molecules of 6OCB. The DFT calculations on isolated molecules of CB6OCB reported in Table II also find this preference of a single *gauche* link for the rotation through $\phi(26)$.

The observed values of $D_{i,j}$ are averages over all the conformations sampled by a flexible molecule; thus [28,48]

$$D_{i,j} = \int_0^{2\pi} P_{LC}(\{\phi(k),n\}) D_{i,j}(\{\phi(k),n\})\, d\{\phi(k),n\}, \qquad (8)$$

where $D_{i,j}(\{\phi(k),n\})$ is the dipolar coupling between nuclei i and j when the molecule is in the conformation n described by the set of bond rotation angles, $\{\phi(k),n\}$, in the liquid-crystal

TABLE II. Energies E_i relative to the all-*trans* form, of conformations, defined by dihedral angles $\phi(k)$ of the alkyloxy chain in CB6OCB calculated by the DFT B3LYP/6-311G** method.

$\phi(k)$ (deg)					
$\phi(25)$	$\phi(26)$	$\phi(27)$	$\phi(28)$	$\phi(37)$	E_i(kJ mol^{-1})
181.4	178.1	179.6	178.4	179.8	0.00
83.3	176.7	181.9	180.3	180.4	6.06
182.2	64.0	180.9	179.1	179.1	−1.11
181.4	177.1	67.9	176.2	180.3	3.65
179.1	178.7	174.8	65.5	175.5	3.23
180.0	180.2	179.3	176.4	65.9	3.77

phase. This averaged dipolar coupling is given by

$$\begin{aligned} D_{i,j}(\{\phi(k),n\}) = &-K_{i,j}\left[r_{i,j}^{-3}(\{\phi(k),n\})\right]S_{zz}(\{\phi(k),n\})[3\cos^2\theta_{ijz}(\{\phi(k),n\})-1] \\ &+[S_{xx}(\{\phi(k),n\}) - S_{yy}(\{\phi(k),n\})][\cos^2\theta_{ijx}(\{\phi(k),n\}) - \cos^2\theta_{ijy}(\{\phi(k),n\})] \\ &+4S_{xy}(\{\phi(k),n\})\cos\theta_{ijx}(\{\phi(k),n\})\cos\theta_{ijy}(\{\phi(k),n\}) \\ &+4S_{xz}(\{\phi(k),n\})\cos\theta_{ijx}(\{\phi(k),n\})\cos\theta_{ijz}(\{\phi(k),n\}) \\ &+4S_{yz}(\{\phi(k)\},n)\cos\theta_{ijy}(\{\phi(k),n\})\cos\theta_{ijz}(\{\phi(k),n\})\}, \end{aligned} \tag{9}$$

where $S_{zz}(\{\phi(k),n\})$, etc., are elements of a conformationally dependent order matrix, $S(\{\phi(k),n\})$ with reference axes xyz fixed in any convenient rigid fragment of the molecule.

Equations (8) and (9) have been used to investigate the conformational distributions of both mesogenic molecules, and dissolved, flexible solutes in uniaxial liquid crystals. To do this requires the adoption of theoretical models for predicting how the order parameters vary with conformation, and crucially to obtain a sufficient number of dipolar couplings, and/or quadrupolar splittings to determine the number of fitting parameters in these theoretical models. This latter condition is not met by the present set of values of D_{CH} obtained from the PELF experiments on CB6OCB, because it has not yet proved possible to assign the observed C-H dipolar splittings at all positions in the spacer. In fact, only the one-bond splitting for C24 can be definitely assigned, which means that there are only five observed couplings (two from the phenyl-C37 and two from the phenyl-O rings, plus $D_{24,29} = D_{24,30}$). The all-*trans* configuration has a plane of symmetry and requires just three order parameters to relate the observed values of these splittings to the order parameters to be expected if the molecule exists only in this fixed conformation. These order parameters, together with the DFT geometry, were then used to calculate the values of $^1D_{CH}$ for all positions in the -O-C_6H_{12}- chain and these are shown in Fig. 21 together with those observed.

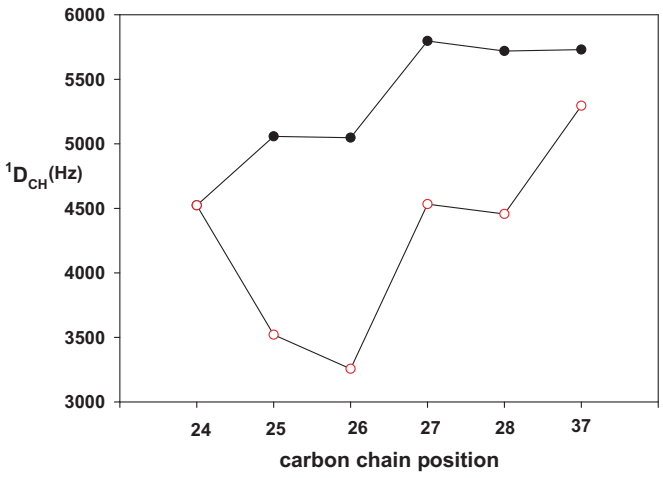

FIG. 21. Observed (○) values of $^1D_{CH}$ for the chain carbon positions in the N_U phase of CB6OCB at 394 K, compared with values calculated (●) for the single, all-*trans* conformation. The assignment of $^1D_{CH}$ at C24 is certain, while those for the other positions are made assuming that the chemical shifts are in the same order in the isotropic and N_U phase.

The order matrix elements calculated for this all-*trans* configuration for axes fixed in the biphenyl-O ring are

$$S_{zz} = 0.56; \quad S_{xx}-S_{yy} = 0.124; \quad S_{xy} = 0;$$
$$S_{xz} = 0.314; \quad S_{yz} = 0.$$

The comparison shown in Fig. 21 clearly demonstrates that in the N_U phase the chain does not exist only in the all-*trans* configuration.

The PELF spectra for the carbons in the hexyloxy chain when the sample is in the N_U phase are compared in Fig. 22 with that recorded for the N_{TB} phase at 377 K. Each -CH_2- group in the chain is prochiral and the two C-H directions in these groups in an enantiomorphic phase are nonequivalent and should show additional splittings in the PELF spectra [13], although their magnitudes may not always be resolvable

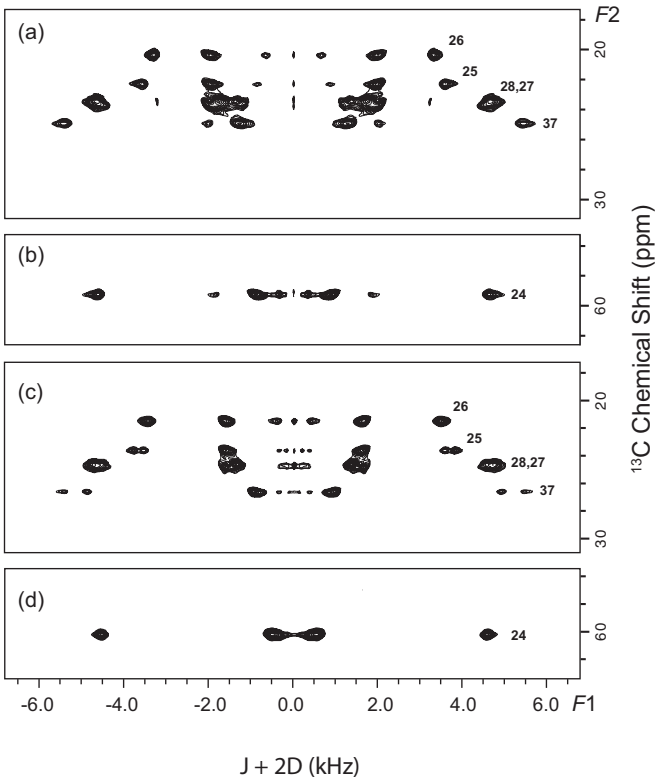

FIG. 22. PELF spectra of the carbon nuclei in the hexyloxy chain in the N_U phase of CB6OCB at 394 K (a,b) compared with the N_{TB} phase at 377 K (c,d). The peak assignments are based on the chemical shifts for a sample in the isotropic phase. The $F1$ axis has been adjusted to allow for the scaling factor of 0.47 introduced by the homonuclear refocusing sequence.

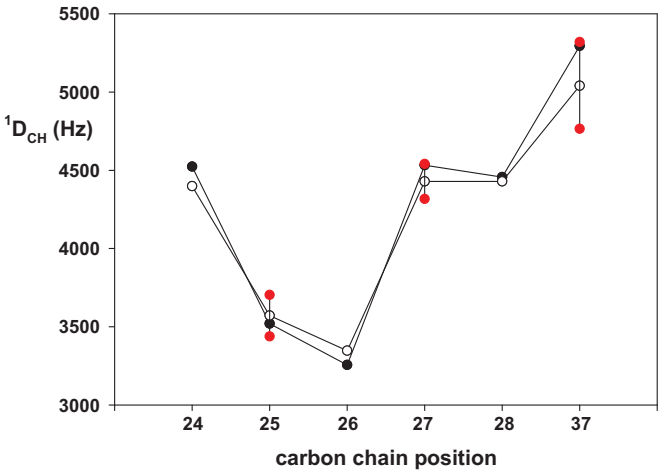

FIG. 23. Comparison of the values of $^1D_{CH}$ observed along the chain at 394 K (N_U) (•) and at 377 K (N_{TB}) (○) for CB6OCB. The assignment of $^1D_{CH}$ at C24 is certain, while those for the other positions are made assuming that the chemical shifts are in the same order in the isotropic and N_U phase. The additional, prochiral splittings at positions C25, C26, and C37 are shown by the red (gray) symbols (•): at these positions the open circles (○) are at the mean splittings.

[16,49]. Such additional splittings are clearly resolved at three positions in the hexyloxy chain, probably at C25, C27, and C37 in the N_{TB} phase, but definitely not for C24 as can be seen in Fig. 22.

Plotting $^1D_{CH}$ experimental values for the chain carbons at 394 K together with those for 377 K, when the sample is in the N_{TB} phase, suggests that the chain conformational distributions in these two phases are very similar (see Fig. 23).

XI. CONCLUSIONS

The data obtained from the one-dimensional (1D) ^{13}C-{^{1}H} and 2D ^{13}C-^{1}H PELF NMR experiments have allowed temperature profiles, S_{zz} (biphenyl-O)(T), and S_{zz} (biphenyl-C)(T), for the two biphenyl arms of CB6OCB to be obtained. At all temperatures in both N_U and N_{TB} phases the order parameter S_{zz}(biphenyl-O) is ∼7% larger than S_{zz}(biphenyl-C). Both order parameters follow the same form of temperature dependence as found for the difluoroterphenyl arms in the symmetric dimer, DTC5C9, in having a maximum value in the N_U phase about 8 °C above the transition to the N_{TB} phase. As we have seen this unusual temperature dependence is consistent with the directors being tilted away from along the direction of the static magnetic field of the spectrometer. When the sample starts to enter the N_{TB} phase there is a biphasic region of ∼2 °C when the ^{13}C-{^{1}H} peaks from both phases are present. The two order parameters show a small, but significant discontinuous decrease of ∼0.01, and the linewidths from C2 and C45 are broadened by approximately threefold.

The PELF splittings proved difficult to assign to specific carbons in the -OC_6H_{12}- chain, but it is possible to show that this chain cannot exist only in the all-*trans* form, and that the conformational distributions in both nematic phases are very similar.

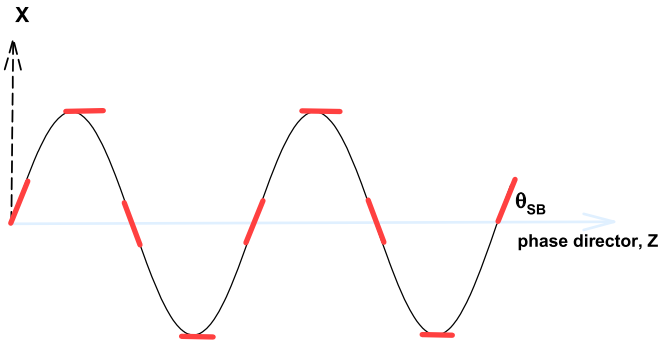

FIG. 24. The directors (red lines) in the splay-bend nematic phase vary in orientation in the range of $0 \pm \theta_{SB}$ in the XZ plane.

The major conclusion concerning the nematic phase of the liquid-crystal dimer CB6OCB is in keeping with that found [15] for the dimer DTC5C9, namely, that the order parameter for the *para* axis passes through a maximum prior to the formation of the N_{TB} phase. It is also of interest to note that the magnitude of this behavior is related to the extent of the nematic phase prior to the formation of the N_{TB} phase. Associated with this is that the strength of the N_{TB}-N_U transition is also related to the nematic range in way analogous to the Sm-A to N systems [41]. The most likely explanation for this unexpected behavior of the order parameter in the nematic phase is that the director is tilted away from the static magnetic field; for the moment it seems sensible to denote this phase as N_X until its structure is clearly established. Our detailed results for the order parameters allow the tilt angle in the N_X phase to be determined and to recognize that it is essentially contiguous with the behavior of the conical angle in the N_{TB} phase. The next challenge is to understand what causes the director to tilt with respect to the static magnetic field of the spectrometer and which axis of the phase is aligned parallel to this.

We have given these difficult questions careful consideration guided in part by the ideas employed by Dozov [3] in developing his theory for the twist-bend and splay-bend nematic phases. This led us to consider the possibility that N_X has strong similarities with the oscillating splay-bend nematic phase; the directors in this phase exhibit a sinusoidal modulation in the XZ plane such that the angle made by a director with the Z axis varies in the range $\pm\theta_{SB}$ as illustrated in Fig. 24 and is achiral.

The starting point adopted by Dozov was the Frank elastic energy of a distorted nematic phase and this was mapped onto a Landau-like theory. This gives the macroscopic free energy F for the two modulated nematic phases as

$$F_{SB} = \left(K_{33}^3\right)/(27CK_{11}) < 0, \tag{10}$$

and

$$F_{TB} = \left(K_{33}^3\right)/(54CK_{22}) < 0. \tag{11}$$

Here K_{11}, K_{22}, and K_{33} are the splay, twist, and bend elastic constants, respectively; C denotes a fourth-order elastic coefficient. For either modulated nematic phase to be stable K_{33} is required to be negative. Further, for the twist-bend nematic to be stable with respect to the splay-bend nematic the inequality $K_{11}/2K_{22} > 1$ needs to be satisfied, and for the

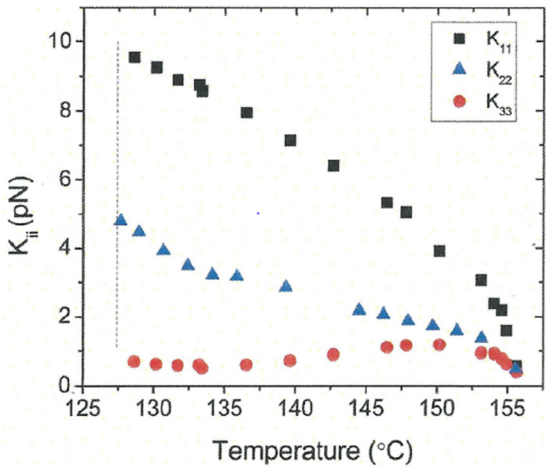

FIG. 25. The temperature dependence of the elastic constants in the nematic phase of the dimer DTC5C7. [Sebastián *et al.*, Phys. Chem. Chem. Phys. **18**, 19299 (2016). Reproduced with permission from the PCCP Owner Societies.]

splay-bend nematic to be stable with respect to the twist-bend nematic requires $K_{11}/2K_{22} < 1$. The theory also predicts the N_{TB}-N_U and N_{SB}-N_U phase transitions, when K_{33} passes through zero, to be second order.

It is useful to place these predictions in an experimental context. Unlike the prediction by Dozov, the N_{TB}-N_U transition is invariably found to be first order in keeping with the symmetries of the N_U and N_{TB} phases [50]. The bend elastic constant in the N_U phase at the transition to the N_{TB} phase is positive, small, and increases slightly [45,51,52]. Contrary to the theoretical prediction K_{33} does not vanish when N_{TB} is formed from the N_U phase but when it is increasing slightly. The inequality $K_{11}/2K_{22} > 1$ is usually satisfied as required for a N_{TB} phase to be formed [45,52], although for a study of the dimer CB7CB this is not so and at the N_{TB}-N transition, $K_{11}/2K_{22} \sim 0.80$ [51]. Of particular significance for our discussion is the temperature dependence of the elastic constants and results have been obtained for DTC5C9 [52], KA(0.2) [20], and DTC5C7 [45]. The results for DTC5C7 are shown in Fig. 25; here the bend elastic constant K_{33} increases after T_{NI} and then decreases to about 0.6 pN at 140 °C before increasing slightly just before the formation of the N_{TB} phase. The ratio $K_{11}/2K_{22}$ is about 1.0 at the N_{TB}-N transition (127 °C) and then grows to 1.24 at 140 °C.

The phase behavior anticipated for DTC5C7 [45], namely, the sequence N_{TB}-N-I is not strictly in accord with the predictions of the model proposed by Dozov and the elastic constants measured for the dimer. In view of this difference in behavior the introduction of a nematic phase which we had previously denoted as N_X is now proposed to be the splay-bend nematic giving the earlier sequence as N_{TB}-N_{SB}-N-I may not be so surprising. The structure of the splay-bend nematic shown in Fig. 24 is biaxial as indeed is the twist-bend nematic phase shown in Fig. 1. The biaxiality of the phase is not revealed by the ^{2}H NMR experiments performed on CB7CB-d_4 [6,24] and CB9CB-d_4 [53]. The reason for this is that the molecular translational diffusion along the helix axis in the N_{TB} phase is sufficiently fast that the biaxiality in the residual quadrupolar tensor of CB7CB-d_4 [23] is averaged to zero. The translational diffusion tensor has yet to be measured for CB6OCB but it is to be expected that the biaxiality in the residual magnetic tensors will indeed be averaged by translational diffusion, especially as in CB7CB-d_4 the diffusion tensor is larger in the nematic phase than the twist-bend nematic phase. The diffusion tensor along the sinusoidal axis should, therefore, be large in the postulated splay-bend nematic phase and the biaxiality in the residual magnetic tensors will be averaged to zero. Although reasonable, this expectation for CB6OCB clearly needs to be tested by experiment [5,25].

However, even though a sequence of three nematic phases has been observed for other dimers with long nematic phases at high temperatures it is clear that more detailed investigations are certainly needed to confirm the existence of the N_{SB} phase prior to the N_{TB} phase. There is clearly a long list of techniques that could be used to look for a phase transition in the nematic phase prior to the formation of the N_{TB} phase with its defining enantiomorphic property. These include techniques such as adiabatic calorimetry, polarizing optical textures, static permittivity, x-ray diffraction, NMR spectroscopy, and birefringence. In addition these techniques and others like resonance x-ray scattering, Raman scattering, and freeze-fracture transmission electron microscopy will also provide valuable information about the structure of the N_X phase.

Consideration should also be given to pretransitional behavior as another possible explanation for the director tilt in the nematic phase prior to the twist-bend nematic phase. Such behavior describes the adoption of defining properties of one liquid-crystal phase by another as the transition linking them is approached. A well-studied example is the transition between the nematic and smectic-A phases. It shows, in particular, that enhancement in the orientational order in the N phase in the vicinity of the transition is associated with smectic-A–like clusters as well as the coupling between the translational and orientational order [54]. This coupling is analogous to that in the Sm-A phase itself and grows with the weakness of the Sm-A to N transition.

It is to be expected that analogous pretransitional behavior would occur at the N_{TB}-N transition, especially in view of the analogy between the Sm-A and N_{TB} phases [55]. The property of particular interest here is the helicoidal structure of the twist-bend nematic phase. This is expected to result in the reduction of the orientational order in the N_{TB} phase with respect to the helicoidal axis and the magnetic field of the NMR spectrometer. In keeping with the pretransitional behavior the orientational order in the nematic phase should decrease as the N_{TB} phase is approached. This will also be in accord with the growth in the molecular clusters with their local N_{TB} structure [55] which should grow with the nematic range and the weakness of the transition.

[1] H. D. Flack, Acta Crystallogr. A **65**, 371 (2009).

[2] T. Sekine, T. Niori, J. Watanabe, T. Furukawa, S. W. Choi, and H. Takezoe, J. Mater. Chem. **7**, 1307 (1997).

[3] I. Dozov, Europhys. Lett. **56**, 247 (2001).

[4] F. C. Frank, in *Proceedings of the International Liquid Crystals Conference, Bangalore,*1979, edited by S. Chandrasekhar (Heyden, London, 1980), pp. 1–6.

[5] Y. Wang, G. Singh, D. M. Agra-Kooijman, M. Gao, H. K. Bisoyi, C. Xue, M. R. Fisch, S. Kumar, and Q. Li, CrystEngComm **17**, 2778 (2015).

[6] M. Cestari, S. Diez-Berart, D. A. Dunmur, A. Ferrarini, M. R. de la Fuente, D. J. B. Jackson, G. R. Luckhurst, M. A. Perez-Jubindo, R. M. Richardson, J. Salud, B. A. Timimi, and H. Zimmermann, Phys. Rev. E **84**, 031704 (2011).

[7] M. Šepelj, U. Baumeister, T. Ivšic, and A. Lesac, J. Phys. Chem. B **117**, 8918 (2013).

[8] P. A. Henderson, and C. T. Imrie, Liq. Cryst. **38**, 1407 (2011).

[9] R. J. Mandle, E. J. Davis, C. T. Archbold, C. C. A. Voll, J. L. Andrews, S. J. Cowling, and J. W. Goodby, Chem. Eur. J. **21**, 8158 (2015).

[10] R. J. Mandle, Soft Matter **12**, 7883 (2016).

[11] R. J. Mandle, C. C. A. Voll, D. J. Lewis, and J. W. Goodby, Liq. Cryst. **43**, 13 (2016).

[12] C. Greco, G. R. Luckhurst, and A. Ferrarini, Soft Matter **10**, 9318 (2014).

[13] L. Beguin, J. W. Emsley, M. Lelli, A. Lesage, G. R. Luckhurst, B. A. Timimi, and H. Zimmermann, J. Phys. Chem. B **116**, 7940 (2012).

[14] S. M. Salili, M. G. Tamba, S. N. Sprunt, C. Welch, G. H. Mehl, A. Jákli, and J. T. Gleeson, Phys. Rev. Lett. **116**, 217801 (2016).

[15] J. W. Emsley, M. Lelli, H. Joy, M.-G. Tamba, and G. H. Mehl, Phys. Chem. Chem. Phys. **18**, 9419 (2016).

[16] R. Amaranatha Reddy and C. Tschierske, J. Mater. Chem. **16**, 907 (2006).

[17] A. G. Vanakaras and D. J. Photinos, Soft Matter **12**, 2208 (2016).

[18] J. W. Emsley, M. Lelli, A. Lesage, and G. R. Luckhurst, J. Phys. Chem. B **117**, 6547 (2013).

[19] I. Miglioli, C. Bacchiocchi, A. Arcioni, A. Kohlmeier, G. H. Mehl, and C. Zannoni, J. Mater. Chem. C **4**, 9887 (2016).

[20] D. A. Paterson, M. Gao, Y.-K. Kim, A. Jamaldi, K. L. Finley, B. Robles-Hernández, S. Diez-Berart, J. Salud, M. R. de la Fuente, B. A. Timimi, H. Zimmermann, C. Greco, A. Ferrarini, J. M. D. Storey, D. O. López, O. L. Lavrentovich, G. R. Luckhurst, and C. T. Imrie, Soft Matter **12**, 6827 (2016).

[21] K. Adlem, M. Čopič, G. R. Luckhurst, A. Mertelj, O. Parri, R. M. Richardson, B. D. Snow, B. A. Timimi, R. P. Tuffin, and D. Wilkes, Phys. Rev. E **88**, 022503 (2013).

[22] J. W. Emsley, P. Lesot, G. De Luca, A. Lesage, D. Merlet, and G. Pileio, Liq. Cryst. **35**, 443 (2008).

[23] G. de Luca, J. W. Emsley, A. Lesage, and D. Merlet, Liq. Cryst. **39**, 211 (2012).

[24] M. Cifelli, V. Domenici, S. V. Dvinskikh, G. R. Luckhurst, and B.A. Timimi, Liq. Cryst. **44**, 204 (2017).

[25] J. W. Emsley, T. J. Horne, G. Celebre, M. Longeri, and H. Zimmermann, J. Phys. Chem. **96**, 1929 (1992).

[26] G. Celebre, G. De Luca, M. Longeri, and J. W. Emsley, J. Phys. Chem. **96**, 2466 (1992).

[27] J. W. Emsley, T. J. Horne, H. Zimmermann, G. Celebre, and M. Longeri, Liq. Cryst. **7**, 1 (1990).

[28] J. W. Emsley, G. R. Luckhurst, and C. P. Stockley, Mol. Phys. **44**, 565 (1981).

[29] J. W. Emsley, G. De Luca, G. Celebre, and M. Longeri, Liq. Cryst. **20**, 569 (1996).

[30] J. W. Emsley, G. De Luca, A. Lesage, D. Merlet, and G. Pileio, Liq. Cryst. **34**, 1071 (2007).

[31] J. Xu, K. Fodor-Csorba, and R. Y. Dong, J. Phys. Chem. A **109**, 1998 (2005).

[32] R. Y. Dong, S. Kumar, and J. Zhang, Chem. Phys. Lett. **448**, 54 (2007).

[33] M. Hong, A. Pines, and S. Calderelli, J. Phys. Chem. A **100**, 14815 (1996).

[34] S. Calderelli, M. Hong, L. Emsley, and A. Pines, J. Phys. Chem. A **100**, 18696 (1996).

[35] See Supplemental Material at http://link.aps.org/supplemental/10.1103/PhysRevE.96.062702 for the results from the DFT calculations.

[36] J. W. Emsley, G. R. Luckhurst, and B. A. Timimi, Chem. Phys. Lett. **114**, 19 (1985).

[37] P. J. Barnes, A. G. Douglass, S. K. Heeks, and G. R. Luckhurst, Liq. Cryst. **13**, 603 (1993).

[38] G. R. Luckhurst, C. Zannoni, P. L. Nordio, and A. Segre, Mol. Phys. **30**, 1345 (1975).

[39] I. Haller, Prog. Solid State Chem. **10**, 103 (1975).

[40] J. P. Jokisaari, G. R. Luckhurst, B. A. Timimi, J. Zhu, and H. Zimmermann, Liq. Cryst. **42**, 708 (2015).

[41] C. T. Imrie, and G. R. Luckhurst, Liquid Crystal Dimers and Oligomers, in *Handbook of Liquid Crystals*, 2nd ed., edited by J. W. Goodby, P. J. Collings, T. Kato, C. Tschierske, H. F. Gleeson, and P. Raynes (Wiley-VCH, Weinheim, Germany, 2014), Vol. 7, Part II.

[42] C. Meyer, G. R. Luckhurst, and I. Dozov, Phys. Rev. Lett. **111**, 067801 (2013).

[43] C. Greco, G. R. Luckhurst, and A. Ferrarini, Phys. Chem. Chem. Phys. **15**, 14961 (2013).

[44] C. Meyer, G. R. Luckhurst, and I. Dozov, J. Mater. Chem. C **3**, 318 (2015).

[45] N. Sebastián, M. G. Tamba, R. Stannarius, M. R. de la Fuente, M. Salamonczyk, G. Cukrov, J. Gleeson, S. Sprunt, A. Jákli, C. Welch, Z. Ahmed, G. H. Mehl, and A. Eremin, Phys. Chem. Chem. Phys. **18**, 19299 (2016).

[46] M. Cestari, E. Frezza, A. Ferrarini, and G. R. Luckhurst, J. Mater. Chem. **21**, 12303 (2011).

[47] J. W. Emsley, P. Lesot, G. R. Luckhurst, A. Meddour, and D. Merlet, Phys. Rev. E **87**, 040501(R) (2013).

[48] J. W. Emsley and G. R. Luckhurst, Mol. Phys. **41**, 19 (1980).

[49] J. W. Emsley, P. Lesot, J. Courtieu, and D. Merlet, Phys. Chem. Chem. Phys. **6**, 5331 (2004).

[50] D. O. López, B. Robles-Hernández, J. Salud, M. R. de la Fuente, N. Sebastián, S. Diez Berart, X. Jaen, D. A. Dunmur, and G. R. Luckhurst, Phys. Chem. Chem. Phys. **18**, 4394 (2016).

[51] C.-J. Yun, M. R. Vengatesan, J. K. Vij, and J.-S. Song, Appl. Phys. Lett. **106**, 173102 (2015).

[52] G. Cukrov, Y. M. Golestani, Y. Xiang, Yu. A. Nastishin, Z. Ahmed, C. Welch, G. H. Mehl, and O. D. Lavrentovich, Liq. Cryst. **44**, 219 (2017).

[53] A. Hoffmann, A. G. Vanakaras, A. Kohlmeier, G. H. Mehl, and D. J. Photinos, Soft Matter **11**, 850 (2015).

[54] S. Yildiz, H. Özbek, C. Glorieux, and J. Thoen, Liq. Cryst. **34**, 611 (2007).

[55] I. Dozov and C. Meyer, Liq. Cryst. **44**, 4 (2017).